RSC Advances

PAPER

View Article Online
View Journal | View Issue

Cite this: *RSC Adv.*, 2021, **11**, 5548

Access to thermally robust and abrasion resistant antimicrobial plastics: synthesis of UV-curable phosphonium small molecule coatings and extrudable additives†

Joseph Bedard, Alexander Caschera and Daniel A. Foucher *

The threat of antibiotic-resistant, biofilm-forming bacteria necessitates a preventative approach to combat the proliferation of robust, pathogenic strains on "high touch surfaces" in the food packaging, biomedical, and healthcare industries. The development of both biocide-releasing and tethered, immobilized biocide surface coatings has risen to meet this demand. While these surface coatings have demonstrated excellent antimicrobial efficacy, there are few examples of antimicrobial surfaces with long-term durability and performance. To this end, UV-curable phosphoniums bearing benzophenone anchors with either an alkyl, aryl, or fluoroalkyl group were synthesized and their efficacy as thermally stable antimicrobial additives in extruded plastics or as surface attached coatings probed. The surface topology and characteristics of these materials were studied to gain insight into the mechanism of their antimicrobial activity. Efficacy against both Gram negative and Gram positive bacteria as either a coating or additive showed compete reductions of the initial bacterial load. Crucially, the materials maintained the ability to kill biofilm-forming bacteria even after being subject to several cycles of abrasion.

Received 21st January 2021
Accepted 26th January 2021

DOI: 10.1039/d1ra00555c

rsc.li/rsc-advances

Introduction

The attachment and proliferation of antibiotic resistant, biofilm-forming bacteria to frequently handled material surfaces has emerged as a public concern, particularly in the biomedical and healthcare industries.[1–6] These "superbug" strains have been attributed to the continued rise in healthcare associated infections (HCAIs), placing a heavy burden on healthcare systems.[7–9] This has been compounded by the over-prescription of antibiotics and overuse of common disinfectants at sub-lethal concentrations,[10] necessitating a modern, preventative approach. Recent advances in the development of biocide-releasing and tethered biocide surfaces have positioned antimicrobial materials as an attractive solution to this challenge.[11–14] Biocide-releasing surfaces, while in some cases effective as a short-term antimicrobial solution, require cell uptake to disrupt protein synthesis, the bacterial membrane or metabolic pathways; all modes of action susceptible to drug resistance.[15] The temporal nature of these surfaces also gives rise to release of non-lethal antimicrobial concentrations at the end of the material lifetime[16] which have been shown to actually enhance the horizontal gene transfer process by which microbiota acquire antibacterial resistance.[10,17]

Tethered cationic biocides have been shown to have excellent antimicrobial efficacy in a variety of simulated environments.[18–21] A tethered approach is advantageous as it greatly reduces initial microbial attachment *via* mechanophysical modes of action, hypothesized to function as a long chain "polymeric spacer" or a charge-based "phospholipid sponge".[19,22,23] While these immobilized cationic surface coatings have exceptional antimicrobial capacities, few possess this property in conjunction with substantial durability to abrasion and other stressors, highlighting a limitation of these coatings.[24–27] Harney and coworkers carried out exploratory studies using tuneable amphiphilic ammonium antimicrobials as solution blended additives in polyurethane.[28] This methodology can yield antimicrobial additives that are surface proximate or more evenly blended in the sample depending on the amphiphobic nature of the cation. The substrate scope tested by these workers was limited to hydrophilic polyurethane resins, and migration to the polymer–air interface was said to be facilitated solely by the hydrophobic nature of the antimicrobials.[28] An example of extruded plastics with antimicrobial properties was reported by Efrati and coworkers, where a blend of essential oils and ammonium functionalized-clay particulate acted as an antimicrobial agent, demonstrating efficacy as a biocide-releasing agent against *E. coli*.[29]

Department of Chemistry and Biology, Ryerson University, 350 Victoria Street, Toronto, Ontario, M5B-2K3, Canada. E-mail: daniel.foucher@ryerson.ca

† Electronic supplementary information (ESI) available: All experimental detail, molecular characterization data. See DOI: 10.1039/d1ra00555c

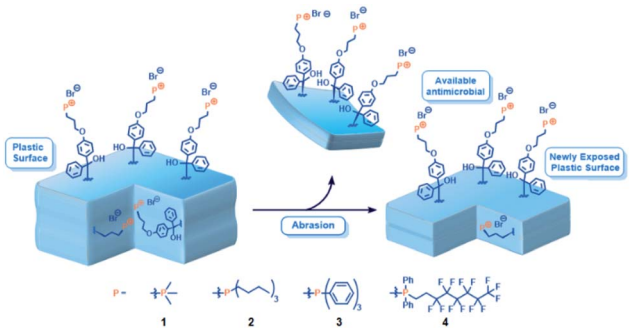

Fig. 1 Schematic showing a cross section of antimicrobial-enriched plastic with sub-surface phosphonium, which upon abrasion is exposed and available to combat microbial growth.

While efforts to develop antimicrobials have centered on the inclusion of ammonium groups,[30–32] less studied are their phosphonium analogs. Phosphonium antimicrobials have been shown to have advantages beyond just antimicrobial efficacy, including low toxicity to mammalian cells and heat resistance.[33–37] High thermal stability, in particular, is an essential requirement of any additive or component of materials fabricated *via* a thermal extrusion process. In the 1990s Kanazawa and co-workers reported surface-attached phosphonium polymer films prepared from the graft polymerization of vinylbenzylchloride (VBC) onto a polypropylene (PP) surface in the presence of photoinitiated free benzophenone. The grafted polymers were functionalized to phosphonium salts *via* surface quaternization with tributyl- or trioctylphosphine and demonstrated antimicrobial efficacy against Gram-positive and Gram-negative bacteria.[34] Recently, we described the preparation of contact active polystyrenic phosphonium coatings grafted to plastic substrates that were robust to mechanical wear and showed efficacy towards pathogenic bacteria.[38]

In this work, we envisioned a class of small molecule, contact-active phosphonium antimicrobial additives introduced at a low loading (*ca.* 1–2 wt%) in thermoplastics resins. The incorporation of an amphiphobic moiety was anticipated to promote surface migration of additives to the polymer–air interface. A UV-active benzophenone group facilitates covalent attachment[39] of the phosphonium-bearing molecular scaffold to either the surface of the plastic or to subsurface layers within the bulk thermoplastic polymer (Fig. 1).

Experimental

General materials and procedures

Detailed synthetic procedures describing the preparation of phosphoniums **1–4** and any intermediates are included in the ESI.† All syntheses, unless otherwise stated, were carried out using standard Schlenk and glovebox protocols. Unless otherwise noted, solvents were purified *via* a solvent purification system (SPS). Polystyrene (PS) coupons were cut from weigh boats (cat. 89106-754) supplied by VWR International, and PS and PP beads used in extrusion were donated by Electro-Pack Inc. LEXAN-brand polycarbonate (PC) was sourced from Lowe's (cat. 1PC0028A). All reagents were purchased from commercial sources and used as received unless otherwise noted. (Perfluorohexyl)ethylene was purchased from Oakwood chemicals and degassed *via* a freeze–pump–thaw (FPT) method (4 cycles). Sodium hydroxide (NaOH, 1 M), 10% aqueous ammonium chloride (NH_4Cl), and 3 M hydrochloric acid (HCl) were sparged with N_2 (g) for 1 h before use. Acetonitrile (MeCN) was dried over 4 Å molecular sieves for 48 h prior to use. 2,2′-Azobis(2-methylpropionitrile) (AIBN) was recrystallized 2× from MeOH. Column chromatography was carried out on silica gel (silica gel 60, 40–63 μm, EMD). Chromatographic purifications were monitored by thin layer chromatography (TLC). Silica-coated aluminum plates (Alugram Sil G/UV254, Macherey-Nagel) were used for TLC tests. Plates were visualized by UV light or $KMnO_4$ staining. Nuclear magnetic resonance (NMR) experiments were carried out on a 400 MHz Bruker Avance II Spectrometer using $CDCl_3$ or C_6D_6. ^{1}H NMR (400 MHz) and ^{13}C $\{^1H\}$ NMR (100.6 MHz) spectra were referenced to the residual proton and central carbon peak of the solvent. ^{31}P $\{^1H\}$ and ^{19}F $\{^1H\}$ spectra were referenced to external standards, 85% H_3PO_4 (δ (^{31}P) = 0.00 ppm), and $CFCl_3$ (δ (^{19}F) = 0.00 ppm), respectively. All chemical shifts are given in δ (ppm) relative to the solvent and assigned to atoms on basis of available 2D spectra for each compound. High resolution mass spectrometry (HRMS) for novel small molecules was carried out using electrospray ionization time of flight (ESI-TOF) and Direct Analysis in Real Time (DART) at the Advanced Instrumentation for Molecular Structure (AIMS) laboratory at the University of Toronto.

Coating preparation

Coating of plastic test samples, which consisted of 6.25 cm^2 ± 1 cm^2 coupons of each plastic material, was performed *via* an ESS AD – LG electrospray apparatus set to 125 kPa that applied the compound uniformly over the test surfaces. UV curing of phosphonium-coated PS and antimicrobial phosphonium-containing plastics was performed using a Novacure spot curing system, supplied from a mercury-arc discharge lamp, at a peak intensity of 5000 mW into a reflective curing chamber 6.5 cm from the light guide source giving a 0.164 W cm^{-2} intensity giving an approximate 10 J cm^{-2} total dose as measured using an EIT UV Power Puck 2.

Co-extrusion of phosphonium-containing plastics

Plastic beads were placed in a 500 mL round bottom flask (RBF) and 1% (w/w) of the active phosphonium was added. EtOH was added to dissolve the compound and the solvent was removed *via* rotary evaporation, adsorbing the phosphonium to the beads. Once dry, the coated beads were then cured using the Novacure spot curing system under the same parameters utilized for the coated networks. Antimicrobial plastics (PP, PS) were extruded into a stainless-steel mold using a hand press thermal extruder donated by Electro-Pack Inc., with the die temperature set to 220 °C and the mold heated in a vacuum oven at 110 °C.

Surface characterization of antimicrobial materials

Advancing water contact angle θ_C images of treated and untreated surfaces were taken using a Teli CCD camera equipped with a macro lens attached perpendicular to the sample surface. The camera was connected to a monitor using a Sony CMA-D camera adapter. Contact angle measurements were performed using SCA20 contact angle software by Data Physics Corporation. Contact angle experiments performed in accordance with ASTM D7334, and images and measurements were taken 30 s after placing the water droplet on the surface. Surface charge densities were measured by submerging the coated PS pieces with 4 cm^2 of coated surface in 1% (w/v) aqueous fluorescein solutions.[30,39] After being submerged overnight in the solution, the coated pieces were rinsed with water until the rinse solution was clear, and then sonicated for 20 min in 9 mL of CTAB and 1 mL of 0.1 M PBS to liberate bound fluorescein into solution. UV-Vis was performed on the solutions at λ = 501 nm to quantify the number of fluorescein molecules in solution, and thus the number of phosphonium charges available on the coated substrate. Surface charge density results (Table 1) were calculated using the Beer–Lambert law with a path length of 1 cm and an extinction coefficient (ε_{501}) of 77 000 M^{-1} cm^{-1} (eqn (1) and (2)).

$$C_{\text{Fluorescein}}\ (\text{mol L}^{-1}) = A_{501}/\varepsilon_{501}\ (\text{M}^{-1}\ \text{cm}^{-1}) \times L\ (\text{cm}) \quad (1)$$

$$[\text{P}^+] = \frac{C_{\text{Fluorescein}}\ (\text{mol L}^{-1}) \times V\ (L) \times N}{A\ (\text{cm}^2)} \quad (2)$$

Atomic force microscopy (AFM) was performed using an Anasys nanoIR2 equipped with Contact Mode NIR2 Probes (resonance frequency 13 ± 4 kHz, spring constant 0.07–0.4 N m^{-1}) at the Ontario Centre for Characterization of Advanced Materials (OCCAM). PC samples were prepared by putting a piece of 3 M Scotch© tape on one half of the sample, coating and curing the sample, and subsequently removing the tape to create a coated and uncoated side. AFM data was processed using Gwyddion 2.48. The preparation of samples for XPS experiments and the XPS experiments themselves were performed at OCCAM.

Antimicrobial testing using the large drop inoculum method

Bacterial test species were grown overnight in 10 mL of 3 g L^{-1} tryptic soy broth (EMD Millipore) at 30 °C (*Arthrobacter* sp.) 37 °C (*E. coli*) within a shaking incubator (125 rpm), and cultures were washed twice *via* centrifugation at 9000 × *g* to replace the growth media with 4 mL of sterile water. *Arthrobacter* sp. (IAI-3), a Gram-positive bacterium originally isolated from indoor laboratory air was inoculated onto all treated and control test surfaces as the model organism for bacterial survival on solid surfaces. Lab strains of Gram-negative *Escherichia coli* (ATCC 11229) was also tested on treated materials. These strains were chosen since they are well characterized and are present in biofilms found within healthcare associated environments.[40,41] The large drop inoculum (LDI) method was used to assess the antimicrobial efficacy of the antimicrobial treatment at a solid–air interface and is a modification of the ISO 22196/JIS Z 2801 standard procedure.[42] Bacterial test species were grown overnight in 3 g L^{-1} tryptic soy broth at 30 °C within a shaking incubator (125 rpm). On the day of testing, 2 mL of growth culture was washed twice by centrifugation at 9000 × *g*, replacing the growth media with 4 mL of sterile water (City of Toronto, Canada), diluting to ~10^7 cells mL^{-1}, and survival on the sample determined by spot plating 100 mL aliquots of these bacterial suspensions in sterile water, described as following. For *Arthrobacter* sp., the inoculated droplets were naturally air-dried within a class II, type A2 biosafety cabinet (Model 3440009, Labconco Corp.) to avoid contamination, and surviving cells were enumerated upon drying, which took 3 h. *E. coli* samples were dried in a Petri dish with lid closed, over a period of 24 h. Enumeration was performed by rehydrating and vortexing samples in 5 mL of a 0.9% saline retrieval solution, which was then serially diluted and spot-plated onto 3 g L^{-1} tryptic soy agar. Plates were then incubated at 25 °C for a period of 3–5 d which allowed for visualization of colony forming units (CFU). At each time point, bacterial survival on the treated samples was compared to survival on triplicate untreated control surfaces of the same material.

Abrasion and antimicrobial testing of abraded plastics

Abrasion of the extruded PP samples was done according to ASTM D5402-19.[43] After LDI testing, the samples were removed from the 50 mL falcon tubes, rinsed with distilled water, and vortexed again in a 50 mL falcon tube containing 15 mL 0.9% saline solution. The samples were rinsed with distilled water again, dried, placed in the biosafety cabinet and sterilized with UV light for 10 min. The sterilized pieces were placed on a scale and rubbed 50 times using cotton cloth saturated with distilled

Table 1 Advancing water contact angle (θ_C) measurements and surface charge density of UV cured phosphonium coatings on plastics

Coating	Surface charge density[a] (PS) × 10^{15} ($[P^+]$ cm^{-2})	θ_C[a] (deg., PC)	Coating thickness[a] (nm, PC)	RMS roughness (nm, PC)
None	N/A	89 ± 3	N/A[b]	3
1	(1.60 ± 0.03)	72 ± 5	N/A[b]	N/A[b]
2	(3.89 ± 0.50)	36 ± 11	47 ± 11	55
3	(2.90 ± 0.20)	64 ± 6	94 ± 38	32
4	(2.95 ± 0.05)	68 ± 2	105 ± 13	36

[a] All measurements performed in triplicate. [b] Not performed.

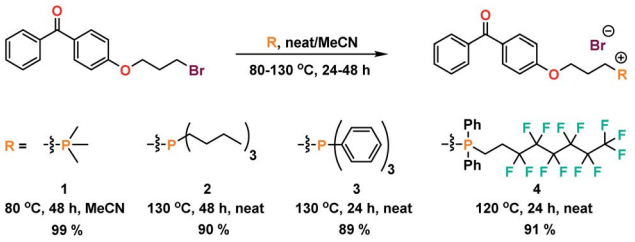

Scheme 1 Menshutkin-like quaternization to yield phosphoniums 1–4.

water. One rub was counted as a back-and-forth motion with consistently applied pressure resulting in a reading between 1.0 and 1.6 kg on a top loading balance. After rubbing, the pieces were once again sterilized in the biosafety cabinet for 10 min, after which they were subject to the LDI protocol.

Results and discussion

Preparation of phosphonium small molecules

Typical extrusion or additive manufacturing processes require high temperatures (>200 °C), and as such phosphonium materials predicted to have good thermal stability were targeted. The methyl, *n*-butyl, phenyl, and fluoroalkyl phosphoniums (**1**, **2**, **3**, and **4**) were chosen to represent varying degrees of hydrophobicity, oleophobicity, and steric bulk. Compounds **1–4** were synthesized in good yields utilizing a Menshutkin-type quaternization procedure with 4-(bromopropoxy)benzophenone (Scheme 1).

UV-initiated grafting of phosphonium coatings to plastic surfaces

Phosphonium coatings were obtained by dissolving **1**, **2**, **3**, or **4** in ethanolic solutions and spray coating onto plastic (*i.e.* PS, PP, PC), followed by a subsequent UV-curing step. Surface charge analysis of these coatings (Tables 1 and S3†) on PS coupons revealed that each of the phosphonium-based coatings had measured surface charge densities on the order of 10^{15} [P^+] cm^{-2}, within the same magnitude of charge densities measured for analogous small molecule ammonium-based coatings.[13,30] Charge density values for coatings comprising **2**, **3** or **4** were within the proposed charge density threshold (>2.5 × 10^{15} [P^+] cm^{-2}) established independently by Murata and Kügler[31] for antimicrobial efficacy against biofilm-forming bacteria. Despite deploying identical coating and curing conditions to the other phosphonium small molecules, the surface charge measurement for the PMe_3 analogue **1** (Table 1) fell outside of the prescribed range and was not further evaluated.[30,31]

Advancing water contact angle (θ_C) measurements (Fig. 2 and Table 1) were performed on the PC coated coupons and were found to trend downward with increasing charge density. The lower surface charge on the coating derived from PMe_3 (**1**) is unexpected, as the networks formed during UV-curing should have similar or higher hydrophilicity than those derived from *n*-Bu (**2**) and Ph (**3**).[37] It is possible that supramolecular network

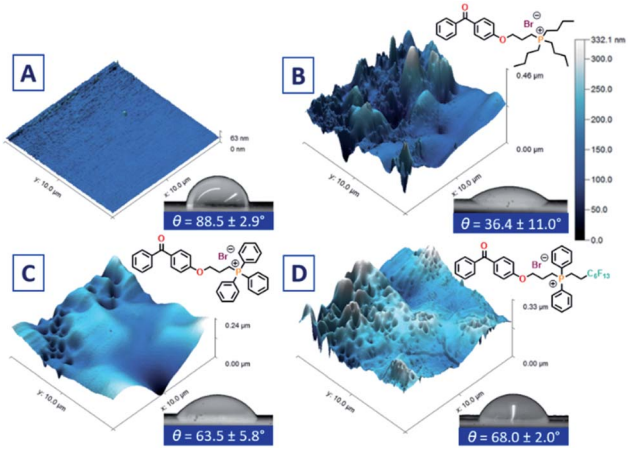

Fig. 2 AFM images and corresponding θ_C image and values of (A) untreated PC plastic; (B) PC treated with **2**; (C) PC treated with **3**, and (D) PC treated with **4**.

growth has been stunted in coatings of **1** by the relatively few sites for hydrogen abstraction on the methyl groups. The incorporation of a fluoroalkyl group in **4** did not significantly alter the hydrophilicity of the coating; a property thought to be a factor in the kill mechanism for antimicrobial coatings.[44,45] Thus, the increased hydrophilicity imparted by a coating prepared with **2** (*n*-Bu) compared to **3** (Ph) may be a consequence of enhanced surface roughness.[46–48]

Atomic force microscopy (AFM) was used to further probe the surface topography of the cured coatings (Fig. 2). While it has been reported that there are limitations of benzophenone as a cross-linker in some applications, particularly in hydrogels,[49] previous studies by our group have shown that antimicrobial activity of UV-curable benzophenone-anchored coatings is independent of the non-porous plastic substrate,[13] and to that end, PC was employed as a model plastic due to its rigidity and lack of warping during UV cure. Polycarbonate UV-cured with **2** yielded a coating with an average thickness of 47 (±11) nm with a root mean square (RMS) roughness value of 55 nm, a 42% increase compared to UV cured coatings prepared with **3** (Fig. 2C). Despite identical spray coating parameters, substrates coated and cured with **3** had nearly double the average thickness compared to **2**, suggesting the morphology of the coating is highly dependent on the nature of the phosphonium alkyl/aryl substituents. Increased roughness for coatings of **2** appears to correlate to its higher surface charge measurements. The surface area accessible to the AFM tip may correspond to the surface sites accessible to the fluorescein dye which probes the surface at the molecular level. By contrast, the thicker, but smoother, coatings of **3** may have fewer phosphonium units accessible to the fluorescein dye.

Co-extrusion of phosphonium-containing plastics

Antimicrobial coatings in a healthcare environment are susceptible to abrasion and deactivation by bacterial debris, necessitating sanitation of the surfaces, often by abrasive processes.[50] We hypothesized that the incorporation of

phosphoniums **2**, **3**, and **4** into bulk PP plastic would provide both surface and subsurface concentrations of the substrate-tethered agent. If abrasion removed the surface phosphoniums, new cations from the subsurface would be exposed and become active, extending the lifetime of the antimicrobial action. Antimicrobial materials were fabricated by co-extrusion of phosphoniums **2–4** with PP. In an attempt to achieve a uniform distribution of the additive into PP, solutions of **2**, **3**, and **4** at 1% (w/w) in minimal EtOH were prepared, and virgin PP beads added to the solution followed by rotary evaporation. This provided a uniform coating of the desired antimicrobial additive on the bead surface, which was then UV-cured to immobilize the compound. Following these steps, the coated beads were extruded at 220 °C into a heated mold (100 °C) to yield the tributylphosphonium-containing plastic **PP-2**, triphenylphosphonium modified **PP-3**, and perfluoroalkyl appended **PP-4** as off-white coloured dogbone pieces (Fig. S59†).

The slight discoloration was due to the natural colour of the phosphoniums and was observed prior to UV or heat treatment, and was not a result of these later processes. The effect of incorporating each phosphonium at 1% was quantified by advancing θ_C (Table 2). Relative to virgin molded PP, samples prepared with **2–4** exhibited modest decreases in advancing θ_C (Table 2), consistent with the decrease observed for the coated pieces. There is likely a lower density of accessible phosphonium charge at the extruded plastic surface in comparison to the UV-cured surface coatings, due to the distribution of phosphonium small molecules subsurface or in the bulk thermoplastic scaffold. AFM measurements of the extruded PP surfaces showed significantly increased roughness relative to the coatings on PC, but measurements using **PP-2** as a representative co-extruded sample did not show significant differences between control and co-extruded samples (Fig. S60†) containing the antimicrobial that could be discerned. XPS was employed to probe the phosphonium content at the surface, subsurface, and bulk of selected co-extruded material **PP-4**. Measurements were taken at descending thickness heights (surface, 5, 10, 20 and 50 μm) after the material was abraded by a microtome (Fig. 3C). Peak analysis was done on the P 2p signal in each XPS spectrum (Fig. 3A and B), corresponding to the P 2s peak found in similar cationic phosphonium systems.[51] The peak intensity was sustained from the surface to the 5 μm step height, while there was a significant drop in signal strength at 10 and 50 μm. At 20 μm however, an anomalous increase was observed, suggesting some uneven phosphonium distribution laterally across the sample during the extrusion process. Elemental analysis of the XPS data (Table S4†) showed significant P present at the surface (2.01%); an atomic % of P greater than that of a single molecule of **4** (1.22%). This suggests the quantity of phosphonium **4** atomic composition at the surface was greater than one molecule per unit area surveyed in the XPS scan. A large quantity of F (16.95%) was also indicative of surface migration of **4**. Crucially, the subsurface levels of P at 5 μm were also substantial (1.83%), with a decrease of only 0.18% compared to the surface. Phosphonium content was diminished greatly at 10 μm, but at 20 μm the atomic % of P was nearly equal to the ratio of P in the molecule, representing a large density of charge at the area surveyed. These results suggest there is a significant proportion of charge at subsurface levels, enriching the materials with the potential to maintain potent antibacterial character after abrasion.

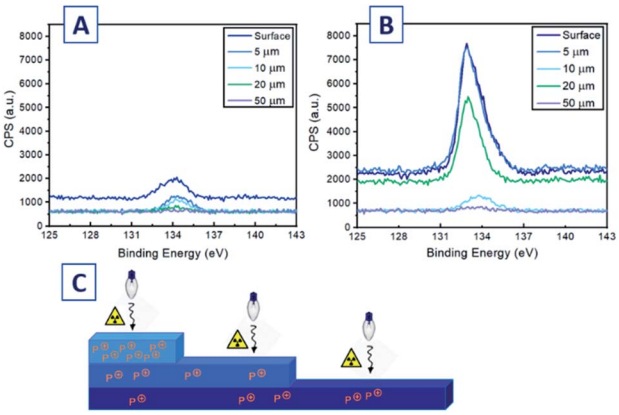

Fig. 3 XPS analysis of co-extruded PP plastics. (A) XPS peak analysis of P 2p peak for a control virgin extruded PP at different step heights. (B) XPS peak analysis of P 2p peak for **PP-4** at different step heights. (C) A schematic of the XPS depth profiling experiment, where pieces were abraded with a microtome to create step heights.

Table 2 θ_C and roughness data for PP co-extruded with UV-curable phosphoniums **2–4**

Material	θ_C[a] (deg.)	RMS roughness (nm)
Extruded PP	88 ± 5	63
PP-2	74 ± 2	91
PP-3	81 ± 1	N/A[b]
PP-4	79 ± 5	N/A[b]

[a] Data measured in triplicate. [b] AFM not performed.

Assessing antimicrobial activity of phosphonium coatings

To establish the antimicrobial efficacy of the novel small molecule phosphonium-based coatings, treated plastic pieces were subjected to the large drop inoculum (LDI) test method previously reported by Ronan *et al.*[40] This method has been shown to be interpretative for determining how antimicrobial coatings function in simulated solid–air interface environments that more closely resemble desiccation processes, to which biofilm-forming bacteria are commonly subjected.[13,40,52] Isolates of *Arthrobacter* sp. (IAI-3) and *Escherichia coli* (ATCC 11229) were chosen as representative Gram-positive and Gram-negative bacterial strains. *Arthrobacter* sp. is a common member of the indoor airborne flora that is continuously deposited on surfaces; this organism has been shown to be vital for the survival and proliferation of multi-bacterial biofilms due to its ubiquity in biofilms and its relevance as a potential human pathogen.[52] Polystyrene coated with phosphoniums **2**, **3**, and **4** exhibited full reductions of viable Gram-positive *Arthrobacter*

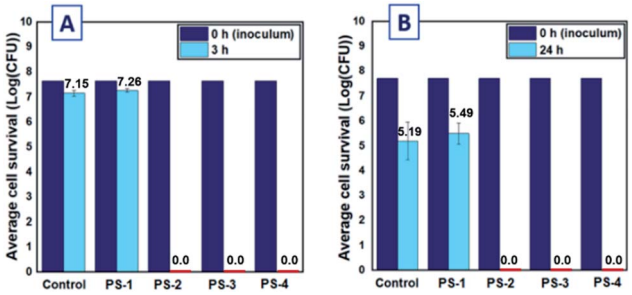

Fig. 4 Average cell survivability of: (A) *Arthrobacter* sp. (IAI-3) and (B) *E. coli* (ATCC strain 11229) against (from left) uncoated PS, and coated PS with **1**, **2**, **3**, and **4**. All testing performed in triplicate. The measurement at 0 h was the initial bacterial load placed on the sample. Red lines denote complete kill.

sp. (Fig. 4A) and Gram-negative *E. coli* cells (Fig. 4B) after 3 and 24 h in contact with the surface, respectively. These coatings possessed significant densities of charged phosphonium, and as such, efficacy against both bacterial cell membrane types is predicted by the phospholipid sponge theory.[32] No threshold for reduction in antimicrobial efficacy was observed for coating roughness or thickness. Only the surface charge-deficient **1** failed to reduce bacterial survival, providing further evidence for the importance of charge density in cationic antimicrobial surface design.

Assessing antimicrobial activity of coextruded phosphonium plastics

A significant challenge to plastics co-extruded with any antimicrobial is having sufficient concentration of the active component at the surface–air interface to effectively kill bacteria. As previously mentioned, XPS analysis of **PP-2** and **PP-4** suggests that the bound phosphoniums self-segregate/aggregate to the plastic–air interface. Fig. 5(A and C) presents the results of the LDI test method for **PP-2**, **PP-3** and **PP-4**

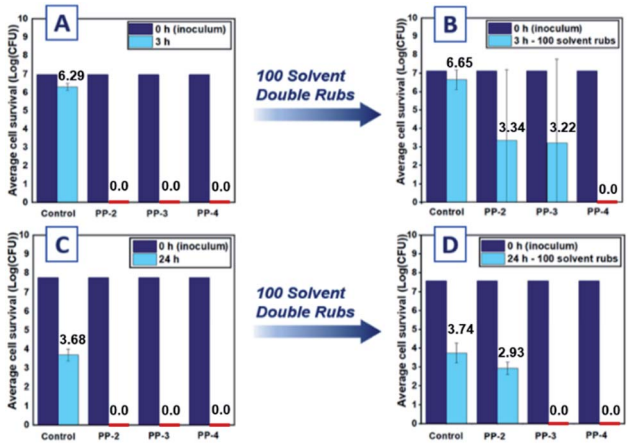

Fig. 5 Average cell viability of: (A) *Arthrobacter* sp. and (C) *E. coli* on (from left) control extruded PP, **PP-2**, **PP-3**, and **PP-4**; (B) *Arthrobacter* sp. on the PP coated samples after 100 cycles of solvent rub abrasion, and (D) *E. coli* on PP coated samples after 100 cycles of solvent rub abrasion. Red lines denote complete kill.

against *Arthrobacter* sp. and *E. coli*. After extrusion and exhaustive washing of the surface with distilled water, the molded pieces exhibited full log reduction of both the *Arthrobacter* sp. (Fig. 5A) and *E. coli* (Fig. 5C) after 3 and 24 h, respectively. This confirms that the extruded samples possessed effective bactericidal concentrations of phosphonium antimicrobial at the surface despite the higher advancing θ_C values relative to their UV-cured coating counterparts.

Abrasion-resistant antimicrobial activity of co-extruded phosphoniums

The antimicrobial performance of these materials against the representative strains of Gram-negative and Gram-positive bacteria lead us to probe the antimicrobial capacity of these materials after being subject to abrasive processes.[52] The "solvent double rub" protocol described in ASTM D540242 (ref. 43) was selected as a representative test of durability, with water chosen as the solvent due to its ubiquity in cleaning solutions. The same extruded PP samples subjected to LDI testing were first rinsed with copious amounts of sterile distilled water, then vortexed for 5 min in saline to remove any bacterial debris from the initial test. After another rinse step, the pieces were subjected to 50 or 100 solvent double rubs on the tested side using a cotton cloth saturated with distilled water, the pressure of each rub measured on a benchtop scale to be between *ca.* 65 kPa and *ca.* 105 kPa (1000 to 1600 g measured for a roughly 1.5 cm^2 surface area). After the double rubs, the pieces were rinsed, sterilized under UV light, and the abraded sides were subject to another inoculation of bacteria. Recent work from our group demonstrated excellent solvent abrasion resistance from polystyrenic spin-coated antimicrobial coatings with pendant tributylphosphonium groups, using a bromophenol blue anionic dye assay to assess durability.[38] After 100 cycles of solvent rub abrasion, the molded antimicrobial plastics **PP-2** and **PP-3** experienced a reduction in efficacy against *Arthrobacter* sp. (Fig. 5A and B), likely corresponding to lower concentrations of phosphonium charge below the plastic surface, exposed after abrasion. For plastics tested against *Arthrobacter* sp., there was large deviation in killing abilities for the triplicate samples of **PP-2** and **PP-3** (Fig. 5B and S62†). The lack of homogeneity in P% laterally across the sample observed by XPS may explain this result: the samples may have a greater concentration of phosphonium at other points on the surface that were not abraded or inoculated with the bacteria. Plastics tested against *E. coli* were successful in inhibiting all bacterial cell growth initially and were subjected to the solvent double rub test for 100 cycles. Abraded **PP-2** exhibited low average reductions of log 0.81 CFU, while abraded **PP-3** killed all the Gram-negative species inoculated onto the surface (Fig. 5D). The reduced efficacy of **PP-2** after the abrasive cycles suggests the observed decrease in P% for **PP-2** relative to **PP-4** still holds. Abraded **PP-4** pieces exhibited full log reductions relative to the control (Fig. 5C), exhibiting broad spectrum antimicrobial efficacy even after abrasion. The **PP-4** sample consistently exhibited full log reductions of both Gram-positive and Gram-negative bacteria in contrast to **PP-2** and **PP-3**, and we attribute this consistency to

improved migration of the fluoroalkyl-containing molecules to the solid–air interface. The effectiveness of **PP-4** in killing these biofilm-forming bacteria far surpasses the durability and abrasion resistance tested for other materials with enhanced durability.[25,53,54]

Conclusions

We have designed a series of UV-curable phosphonium-containing molecules that when applied either as a surface coating or as a co-extrusion additive, demonstrate excellent antimicrobial efficacy against Gram-positive and Gram-negative bacteria. The incorporation of fluoroalkyl tails into the molecular scaffold furnished abrasion resistant antimicrobial phosphonium compounds. Tough, abrasion resistant, low toxicity UV-curable phosphonium coatings/extrusion additives for industrial and medical purposes is now being actively pursued.

Conflicts of interest

There are no conflicts to declare.

Acknowledgements

The authors would like to thank Dr Robert Gossage and Dr Stephen Wylie for editorial help. The authors like to thank J&K Scientific for their ongoing support.

Notes and references

1 E. J. Septimus and M. L. Schweizer, *Clin. Microbiol. Rev.*, 2016, **29**, 201–221.
2 E. Zimlichman, D. Henderson, O. Tamir, C. Franz, P. Song, C. K. Yamin, C. Keohane, C. R. Denham and D. W. Bates, *JAMA Intern. Med.*, 2016, **173**, 2039–2046.
3 D. Pittet and D. C. Angus, *JAMA, J. Am. Med. Assoc.*, 2015, **313**, 365–366.
4 A. P. R. Wilson, D. M. Livermore, J. A. Otter, R. E. Warren, P. Jenks, D. A. Enoch, W. Newsholme, B. Oppenheim, A. Leanord, C. McNulty, C. Tanner, S. Bennett, M. Cann, J. Bostock, E. Collins, S. Peckitt, L. Ritchie, C. Fry and P. Hawkey, *J. Hosp. Infect.*, 2016, **92**, S1–S44.
5 N. Horn and A. K. Bhunia, *Front. Microbiol.*, 2018, **9**, 1–16.
6 M. D. Kirk, S. M. Pires, R. E. Black, M. Caipo and J. A. Crump, *PLoS One*, 2015, **12**, 1–21.
7 S. S. Magill, J. R. Edwards, W. Bamberg, Z. G. Beldavs, G. Dumyati, M. A. Kainer, R. Lynfield, M. Maloney, L. McAllister-Hollod, J. Nadle, S. M. Ray, D. L. Thompson, L. E. Wilson and S. K. Fridkin, *N. Engl. J. Med.*, 2014, **370**, 1198–1208.
8 J. D. Bryers, *Biotechnol. Bioeng.*, 2008, **100**, 1–18.
9 K. Page, M. Wilson and I. P. Parkin, *J. Mater. Chem.*, 2009, **19**, 3819–3831.
10 D. I. Andersson and D. Hughes, *Drug Resist. Updates*, 2012, **15**, 162–172.
11 F. Siedenbiedel and J. C. Tiller, *Polymers*, 2012, **4**, 46–71.
12 R. Ben-Knaz, R. Pedahzur and D. Avnir, *Adv. Funct. Mater.*, 2010, **20**, 2324–2329.
13 L. Porosa, A. Caschera, J. Bedard, A. Mocella, E. Ronan, A. J. Lough, G. Wolfaardt and D. A. Foucher, *ACS Appl. Mater. Interfaces*, 2017, **9**, 27491–27503.
14 R. Yeasmin, H. Zhang, J. Zhu and P. Cadieux, *Prog. Org. Coat.*, 2019, **127**, 308–318.
15 J. Jońca, C. Tukaj, W. Werel, U. Mizerska, W. Fortuniak and J. Chojnowski, *J. Mater. Sci.: Mater. Med.*, 2016, **27**, 1–14.
16 C. Adlhart, J. Verran, N. F. Azevedo, H. Olmez, M. M. Keinänen-Toivola, I. Gouveia, L. F. Melo and F. Crijns, *J. Hosp. Infect.*, 2018, **99**, 239–249.
17 J. Jutkina, N. P. Marathe, C. F. Flach and D. G. J. Larsson, *Sci. Total Environ.*, 2018, **616**, 172–178.
18 A. M. Klibanov, *J. Mater. Chem.*, 2007, **17**, 2479–2482.
19 L. A. T. W. Asri, M. Crismaru, S. Roest, Y. Chen, O. Ivashenko, P. Rudolf, J. C. Tiller, H. C. Van Der Mei, T. J. A. Loontjens and H. J. Busscher, *Adv. Funct. Mater.*, 2014, **24**, 346–355.
20 P. Li, Y. F. Poon, W. Li, H. Zhu, S. H. Yeap, Y. Cao, X. Qi, C. Zhou, M. Lamrani, R. W. Beuerman, E. T. Kang, Y. Mu, C. Li, M. W. Chang, S. S. Jan Leong and M. B. Chan Park, *Nat. Mater.*, 2010, **10**, 2–9.
21 A. Caschera, K. B. Mistry, J. Bedard, E. Ronan, M. A. Syed, A. U. Khan, A. J. Lough, G. Wolfaardt and D. A. Foucher, *RSC Adv.*, 2019, **9**, 3140–3150.
22 J. C. Tiller and C. Liao, *Proc. Natl. Acad. Sci. U. S. A.*, 2001, **98**, 5981–5985.
23 A. M. Bieser and J. C. Tiller, *Macromol. Biosci.*, 2011, **11**, 526–534.
24 I. Cerkez, H. B. Kocer, S. D. Worley, R. M. Broughton and T. S. Huang, *Langmuir*, 2011, **27**, 4091–4097.
25 H. B. Kocer, A. Akdag, S. D. Worley, O. Acevedo, R. M. Broughton and Y. Wu, *ACS Appl. Mater. Interfaces*, 2010, **2**, 2456–2464.
26 G. S. Reddy, M. N. Nadagouda and J. A. Sekhar, *Key Eng. Mater.*, 2012, **521**, 1–33.
27 M. C. Connelly, G. S. Reddy, M. N. Nadagouda and J. A. Sekhar, *Clean Technol. Environ. Policy*, 2017, **19**, 845–857.
28 M. B. Harney, R. R. Pant, P. A. Fulmer and J. H. Wynne, *ACS Appl. Mater. Interfaces*, 2009, **1**, 39–41.
29 R. Efrati, M. Natan, A. Pelah, A. Haberer, E. Banin, A. Dotan and A. Ophir, *J. Appl. Polym. Sci.*, 2014, **131**, 1–10.
30 H. Murata, R. R. Koepsel, K. Matyjaszewski and A. J. Russell, *Biomaterials*, 2007, **28**, 4870–4879.
31 R. Kügler, O. Bouloussa and F. Rondelez, *Microbiology*, 2005, **151**, 1341–1348.
32 J. Gao, E. M. White, Q. Liu and J. Locklin, *ACS Appl. Mater. Interfaces*, 2017, **9**, 7745–7751.
33 A. Kanazawa, T. Ikeda and T. Endo, *J. Polym. Sci., Part A: Polym. Chem.*, 1993, **31**, 335–343.
34 A. Kanazawa, T. Ikeda and T. Endo, *J. Polym. Sci., Part A: Polym. Chem.*, 1993, **31**, 1467–1472.
35 R. Guterman, B. M. Berven, T. Chris Corkery, H. Y. Nie, M. Idacavage, E. R. Gillies and P. J. Ragogna, *J. Polym. Sci., Part A: Polym. Chem.*, 2013, **51**, 2782–2792.

36 T. J. Cuthbert, T. D. Harrison, P. J. Ragogna and E. R. Gillies, *J. Mater. Chem. B*, 2016, **4**, 4872–4883.
37 T. J. Cuthbert, B. Hisey, T. D. Harrison, J. F. Trant, E. R. Gillies and P. J. Ragogna, *Angew. Chem., Int. Ed.*, 2018, **57**, 12707–12710.
38 R. Shum, A. Caschera, S. Lu and D. A. Foucher, *ACS Appl. Bio Mater.*, 2019, **3**, 4302–4315.
39 G. Becker, Z. Deng, M. Zober, M. Wagner, K. Lienkamp and F. R. Wurm, *Polym. Chem.*, 2018, **9**, 315–326.
40 E. Ronan, C. W. Yeung, M. Hausner and G. M. Wolfaardt, *Biofouling*, 2013, **29**, 1087–1096.
41 S. Hota, Z. Hirji, K. Stockton, C. Lemieux, H. Dedier, G. Wolfaardt and M. A. Gardam, *Infect. Control Hosp. Epidemiol.*, 2009, **30**, 25–33.
42 ISO 22196:2011, *Measurement of Antibacterial Activity on Plastics and Other Non-Porous Surfaces*, 2016.
43 ASTM D5402-19, *Standard Practice for Assessing the Solvent Resistance of Organic Coatings Using Solvent Rubs*, 2019.
44 A. M. P. McDonnell, D. Beving, A. Wang, W. Chen and Y. Yan, *Adv. Funct. Mater.*, 2005, **15**, 336–340.
45 I. Francolini, C. Vuotto, A. Piozzi and G. Donelli, *APMIS*, 2017, **125**, 392–417.
46 C. Borgs, J. De Coninck, R. Kotecký and M. Zinque, *Phys. Rev. Lett.*, 1995, **74**, 2292–2294.
47 S. Herminghaus, *Europhys. Lett.*, 2000, **52**, 165–170.
48 L. Cao, H. A. Hu and D. Gao, *Langmuir*, 2007, **23**, 4310–4314.
49 E. K. Riga, J. S. Saar, R. Erath, M. Hechenbichler and K. Lienkamp, *Polymers*, 2017, **9**, 686.
50 W. Hartleb, J. S. Saar, P. Zou and K. Lienkamp, *Macromol. Chem. Phys.*, 2016, **217**, 225–231.
51 R. K. Blundell and P. Licence, *Phys. Chem. Chem. Phys.*, 2014, **16**, 15278–15288.
52 W. Stone, O. Kroukamp, D. R. Korber, J. McKelvie and G. M. Wolfaardt, *Front. Microbiol.*, 2016, **7**, 1–15.
53 S. A. Sattar, C. Bradley, R. Kibbee, R. Wesgate, M. A. C. Wilkinson, T. Sharpe and J. Y. Maillard, *J. Hosp. Infect.*, 2015, **91**, 319–325.
54 J. Gao, N. E. Huddleston, E. M. White, J. Pant, H. Handa and J. Locklin, *ACS Biomater. Sci. Eng.*, 2016, **2**, 1169–1179.